

A Study of Preferential Weld Corrosion in the Presence of Carbon Dioxide and
Acetic Acid

by

Nur Amalia Binti Noor Azmi
14918

Dissertation submitted in partial fulfillment of
the requirements for the
Degree of Engineering (Hons)
(Mechanical)

January 2015

Universiti Teknologi PETRONAS,
32610 Bandar Seri Iskandar,
Perak Darul Ridzuan,
Malaysia.

CERTIFICATION OF APPROVAL

A Study of Preferential Weld Corrosion in the Presence of Carbon Dioxide and Acetic Acid

by

Nur Amilia Binti Noor Azmi

14918

A project dissertation submitted to the
Mechanical Engineering Programme
Universiti Teknologi PETRONAS
in partial fulfillment of the requirement for the
BACHELOR OF ENGINEERING (Hons)
(MECHANICAL)

Approved by,

_____.

(DR KEE KOK ENG)

UNIVERSITI TEKNOLOGI PETRONAS
32610, BANDAR SERI ISKANDAR, PERAK

January 2015

CERTIFICATION OF ORIGINALITY

This is to certify that I am responsible for the work submitted in this project, that the original work is my own except as specified in the references and acknowledgements, and that the original work contained herein have not been undertaken or done by unspecified sources or persons.

NUR AMILIA BINTI NOOR AZMI

ABSTRACT

The presence of carbon dioxide (CO₂) gas in oil and gas steel pipeline is a major concern in the industry. CO₂ gas dissolves in water to form carbonic acid which will further dissociate to form free hydrogen ions that can cause rapid corrosion to steel material. In addition, the presence of organic acid such as acetic acid contributes to the additional sources of free hydrogen ions. What is more critical is the fact that these thousand miles of pipelines are connected through welds, which are very susceptible to galvanic corrosion, causing preferential weld corrosion (PWC). Galvanic corrosion occurs due to the difference in compositions and microstructures of the weldment. The primary objective of this study is to investigate the weldment structure and the microstructures of parent metal region, heat-affected zone and weld metal region of an API 5L X52 grade carbon steel pipe. This study also aims to study the effects of varying pH levels and acetic acid concentrations at elevated temperatures to the corrosion behavior of different weldment regions in the presence of acetic acid and CO₂ corrosion. A welded section of an old API 5L X52 pipe which had been exposed to CO₂ corrosion was used as the test samples in this study. Critical literature review has been done regarding the pipe material, structure of weldment, carbon dioxide and acetic acid corrosion as well as the experimental setup and procedures according to ASTM G5-94 and NACE Standard TM0169-2000. An attainable test matrix has been designed as a guide for the experimental study to achieve the objectives. An electrochemical test by using Linear Polarization Resistance (LPR) was used to conduct the corrosion measurement analysis. Results from Zero Resistance Ammeter (ZRA) show that the weld metal and heat affected zone metal always behave anodically compared to parent metal. Based on the Linear Polarization Resistance, the corrosion rates increased for all three metals due to the acidity level in low pH condition that inhibits the formation of protective film. The corrosion rates also increased in the presence of 1000 ppm acetic acid due to the acidity caused by acetic acid dissociations which provides more hydrogen ions. The data collected are presented and discussed thoroughly with supporting literature review.

Keywords: preferential weld corrosion, CO₂ corrosion, acetic acid, weld, API 5L X52

ACKNOWLEDGEMENT

I would like to express my deepest appreciation to all who provided me the possibility to complete this project. A special appreciation is given to my Final Year Project supervisor, Dr Kee Kok Eng who has guided me throughout the two semesters. I would like to thank the staffs of Center of Corrosion Research (CCR) Universiti Teknologi PETRONAS too, who have given me the opportunity to conduct my experiments in CCR. A special gratitude goes to my family and friends for their supports and advices. Last but not least, I would like to thank everyone who has involved directly and indirectly towards this project.

TABLE OF CONTENTS

CERTIFICATION OF APPROVAL	i
CERTIFICATION OF ORIGINALITY	ii
ABSTRACT	iii
ACKNOWLEDGEMENT	iv
LIST OF FIGURES	vii
LIST OF TABLES	viii
CHAPTER 1: INTRODUCTION	1
1.1 Background Study	1
1.2 Problem Statement	2
1.3 Objectives	3
1.4 Scope Of Study	4
CHAPTER 2: LITERATURE REVIEW	5
2.1 Oil and Gas Pipeline	5
2.2 Weldment Structure	7
2.3 Carbon Dioxide (CO ₂) Corrosion	9
2.3.1 The effect of pH on CO ₂ corrosion	11
2.3.2 The effect of temperature on CO ₂ corrosion	11
2.3.3 The effect of acetic acid (HAc) on CO ₂ corrosion	12
CHAPTER 3: METHODOLOGY	13
3.1 Research Methodology	13
3.1.1 Sample preparation	13
3.1.2 Microstructure analysis	13
3.1.3 Corrosion test and corrosion monitoring analysis	13
3.2 Project Workflow	14
3.3 Gantt Charts And Key Milestones	15
3.4 Test Matrix	17
3.4.1 Linear Polarization Resistance experiment	18
3.5 Sample Preparation	19
3.6 Solution Preparation	22
3.6.1 Calculation for 3% NaCl required	22
3.6.2 Calculation for 1000 ppm acetic acid required	22
CHAPTER 4: RESULT AND DISCUSSION	23
4.1 Microscopy Analysis	23
4.2 Corrosion Currents Of Parent Metal, HAZ Metal and Weld Metal	25
4.3 Corrosion Rates Of Parent Metal, HAZ Metal and Weld Metal	27

4.3.1 Corrosion rates at pH 4 with 0 ppm acetic acid.....	27
4.3.2 Corrosion rates at pH 4 with 1000 ppm acetic acid.....	29
4.3.3 Corrosion rates at pH 6.6 with 0 ppm acetic acid.....	31
4.3.4 Corrosion rates at pH 6.6 with 1000 ppm acetic acid.....	32
4.4 The Effect Of Ph.....	34
4.4.1 Effect of varying pH at 0 ppm acetic acid	34
4.4.2 Effect of varying pH at 1000 ppm acetic acid	36
4.5 The Effect Of Acetic Acid Concentration	37
4.5.1 Effect of varying acetic acid concentration at pH 4.....	37
4.5.2 Effect of varying acetic acid concentration at pH 6.6.....	39
4.6 Summary Of Corrosion Rates	40
CHAPTER 5: CONCLUSION AND RECOMMENDATION	42
5.1 Conclusion.....	42
5.2 Recommendation.....	43
REFERENCES.....	44

LIST OF FIGURES

FIGURE 2.1. The cross-section of a weldment	7
FIGURE 3.1. Project flow chart.....	14
FIGURE 3.2. Original sample of X52 weldment.....	19
FIGURE 3.3. Parent metal, HAZ metal and weld metal regions of a weldment.	19
FIGURE 3.4. Parent metal, HAZ metal and weld metal after sectioning process.	20
FIGURE 3.5. Mounted samples of the working electrodes.	20
FIGURE 3.6. The electrochemical setup.	21
FIGURE 4.1. Microstructure of parent metal at 20X magnification.	23
FIGURE 4.2. Microstructure of HAZ metal at 20X magnification.	24
FIGURE 4.3. Microstructure of weld metal at 20X magnification.	24
FIGURE 4.4. Icorr versus time in 0 ppm and 1000 ppm acid at pH 4.....	25
FIGURE 4.5. Corrosion current versus time in 0 ppm and 1000 ppm acid at pH 6.6.	26
FIGURE 4.6. Corrosion rate versus time at pH 4 with 0 ppm acid.	27
FIGURE 4.7. Corrosion rate versus time at pH 4 with 1000 ppm acid.	29
FIGURE 4.8. Corrosion rates versus time at pH 6.6 with 0 ppm acid.....	31
FIGURE 4.9. Corrosion rates versus time at pH 6.6 with 1000 ppm acid.....	32
FIGURE 4.10. Corrosion rate versus time for pH 4 and pH 6.6 at 0 ppm acid.	34
FIGURE 4.11. Corrosion rates versus time at pH 4 and pH 6.6 in 1000 ppm acid. ..	36
FIGURE 4.12. Corrosion rates versus time with 0 ppm and 1000 ppm acid at pH 4.37	
FIGURE 4.13. Corrosion rates versus time in 0 ppm and 1000 ppm acid at pH 6.6. 39	
FIGURE 4.14. Summary of average corrosion rates.	40

LIST OF TABLES

TABLE 2.1. Mechanical properties of API 5L PSL 2 pipes.....	5
TABLE 2.2. Maximum chemical compositions of API 5L PSL 2 pipes.....	6
TABLE 3.1. FYP I Gantt chart.	15
TABLE 3.2. FYP II Gantt chart.	16
TABLE 3.3. Experimental parameters.....	17
TABLE 3.4. Solution parameters.....	18
TABLE 4.1. Summary of corrosion rates.	40

CHAPTER 1: INTRODUCTION

1.1 Background Study

In oil and gas industry, thousand miles of cross-country pipelines carrying substances are transported in high integrity pipelines connected by welds. Corrosion of weld is among the significant concerns in pipeline welding technology and many studies have been focusing on Preferential Weld Corrosion (PWC). Briefly explained, PWC is a selective and rapid corrosion that occur mainly from galvanic effect due to the difference in compositions and microstructures between weld metal, parent metal and heat-affected zone (HAZ) induced by the welding process [1], [2].

Localized metal loss can occur if the weld metal or the HAZ region is anodic to the parent metal. On the contrary, galvanic corrosion at weld metal can be reduced if the weld metal is selected to be slightly noble than the parent metal. Thus, metal loss can be distributed over the larger area of parent metal. The approach of adding more noble metals such as Nickel (Ni), Chromium (Cr) and Molybdenum (Mo) in order to increase the strength and cathodic potential of weld metal has already been practiced in the industry. However, the addition of alloying elements in the weldment has been reported to cause preferential weld corrosion in ‘sweet environment’ where there is the presence of carbon dioxide, as proven in several studies [2], [3], [4].

In oil and gas industry, ‘sweet environment corrosion’ refers to degradation of metals due to carbon dioxide (CO₂) as the corroding agent. CO₂ corrosion commonly occurs in wet gas line as well as multiphase gas line [5] which usually transport mixture of natural hydrocarbons, gases, organic compounds as well as brine. Popoola et.al [6] stated that CO₂ corrosion is influenced by many factors mainly temperature, pH level, flow condition and metal characteristics. In addition, a study published in 1999 [7] mentioned that the presence of organic acids was found in 1944.

Since then, many studies [5], [7], [8] have been investigating the effect of organic acids in CO₂ corrosion of oil and gas pipelines. According to Popoola et.al [6], CO₂

corrosion usually cause pitting and mesa attack under medium-flow conditions. Such rapid material degradation will result in the loss of mechanical properties of the pipeline such as strength, ductility and impact strength. Consequently, severe corroded pipes will incur expensive replacement, in addition to more loss due to halted production and plant shutdown.

1.2 Problem Statement

Galvanic effect is the main cause of preferential weld corrosion, where heating and cooling of metal during welding process will alter the material composition and microstructure [1]. Despite the addition of alloying elements in the weld metal helps to improve corrosion resistance by shifting the cathodic potential to the parent metal, the practice does not solve localized corrosion of weldment in sweet environment, as reported by Turgoose et.al [2], [3]. Thus it is important to understand the behavior of preferential weld corrosion in order to improve prevention methods.

Sweet environment has always affecting oil and gas industry as CO₂ gas acts as active corroding agents. Dry CO₂ gas is non-corrosive in pipeline system [6]; however the presence of various substances such as water, hydrocarbons, organic compounds and brine produce wet corrosive CO₂. In sweet environment, PWC attack occurs due to the presence of free hydrogen ions resulting from dissolved CO₂ gas as well as dissociation of organic acids. In fact, a study by Gunaltun and Larrey [9] found significant amount of organic acids measured in water samples collected from pipelines affected by wet gas line corrosion, as much as 300 ppm to 2000 ppm. As mentioned earlier [2], [6], many factors also contributing to CO₂ corrosion; mainly temperature, pH level, flow conditions and material characteristics.

1.3 Objectives

The objectives of this study are:

- To investigate weldment structure and microstructures of parent metal region, heat-affected zone and weld metal region of an X52 welded pipe.
- To study the effects of varying pH levels at elevated temperature to the corrosion behavior of weldment regions in the presence of acetic acid and CO₂ corrosion.
- To study the effects of varying acetic acid concentration at elevated temperature to the corrosion behavior of weldment regions in CO₂ corrosion.

1.4 Scope of Study

The scope of this study covers experimental analysis of preferential weld corrosion of Carbon Steel API 5L X 52 pipes welded, exposed to carbon dioxide and acetic acid. The sample was obtained from a welded section of an old pipe that had been exposed to CO₂ corrosion. The effect of elevated temperature, pH level and acetic acid concentration to the corrosion behavior of parent metal region, HAZ region and weld metal region are investigated. As mentioned earlier [1], welding process can affect the microstructures and compositions of weldment, however the effect of applying different welding process is not in this scope of study.

The experiment will be conducted under atmospheric pressure with CO₂ partial pressure at 1 bar. The other various factors of CO₂ corrosion other than pH level and acetic acid concentration are not included in the study scope. The methodology of the study involves electrochemical test using Linear Polarization Resistance (LPR) to analyze the corrosion behavior and corrosion rates of the samples. The objectives of this study are substantial and the expected results will be produced from measurable experimental tests. The study can be accomplished within the allocated time frame. The expected progress and timeline are proposed in the following chapters as illustrated in the Gantt chart and project key milestones.

CHAPTER 2: LITERATURE REVIEW

2.1 Oil and Gas Pipeline

Carbon steel has always been the material of choice for oil and gas pipelines due to its availability and relatively low cost than other corrosion-resistant alloys [8]. Furthermore, carbon steel pipe has high strength and excellent weldability to ensure strong seals especially for hundreds-mile pipelines. One of the most widely used standards is the American Petroleum Institute (API) Specification 5L, which covers comprehensive specifications mainly developed for pipelines in oil and gas industry. According to API Specification 5L released in 2004 [10], the purpose of the specification is to provide standards for pipe suitable for use in transporting gas, water and oil. There are two product specification levels (PSL); PSL1 and PSL2 followed by manufacturers to meet the requirement for oil and gas pipeline manufacturing. Table 2.1 shows the mechanical properties and Table 2.2 shows the chemical compositions of API 5L PSL2 pipes [10].

TABLE 2.1 Mechanical properties of API 5L PSL 2 pipes [10].

Grade	Minimum yield strength		Minimum ultimate tensile strength	
	psi	MPa	psi	MPa
B	35 000	241	60 000	414
X42	42 000	290	60 000	414
X46	46 000	317	63 000	434
X52	52 000	359	66 000	455
X56	56 000	386	71 000	490
X60	60 000	414	75 000	517
X65	65 000	448	77 000	531
X70	70 000	483	82 000	565
X80	80 000	552	90 000	621

TABLE 2.2. Maximum chemical compositions of API 5L PSL 2 pipes [10].

Grade	Carbon, Maximum (wt %)	Manganese, Maximum (wt %)	Phosphorus, Maximum (wt %)	Sulfur, Maximum (wt %)	Titanium, Maximum (wt %)
Seamless					
B	0.24	1.20	0.025	0.015	0.04
X42	0.24	1.30	0.025	0.015	0.04
X46, X52, X56, X60	0.24	1.40	0.025	0.015	0.04
X65, X70, X80	0.24	1.40	0.025	0.015	0.06
Welded					
B	0.22	1.20	0.025	0.015	0.04
X42	0.22	1.30	0.025	0.015	0.04
X46, X52, X56	0.22	1.40	0.025	0.015	0.04
X60	0.22	1.40	0.025	0.015	0.04
X65	0.22	1.45	0.025	0.015	0.06
X70	0.22	1.65	0.025	0.015	0.06
X80	0.22	1.85	0.025	0.015	0.06

2.2 Weldment Structure

During welding process, a combination of heat source being applied to the material and the use of electrode with different chemical composition usually caused the weld joint to have many microstructurally distinct regions identified as the fusion zone, the unmixed region, the partially melted region, the heat-affected zone, and the unaffected base metal [11]. The cross-section of a weldment is shown in Figure 2.1.

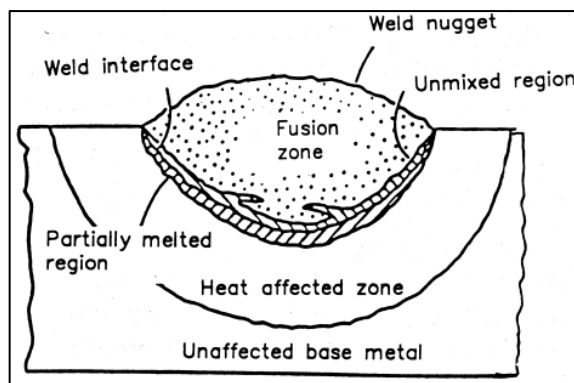


FIGURE 2.1. The cross-section of a weldment [11].

The unmixed region is a part of fusion zone and is actually the melted base metal that has quickly solidified and has the same composition as the base metal. Since it is a fusion of base metal and filler metal with different chemical compositions, this region exhibits compositional and microstructural heterogeneities. For instance, an observable concentration of nickel and chromium can be found in the composition of weld metal region when a nickel and chromium is added in the filler metal for the purpose of increasing cathodic potential of weld metal [11].

The partially melted zone is usually one or two grains into the heat-affected zone and thus is a part of HAZ region. The heat-affected zone is the unmelted region that has experienced high temperature able to produce microstructural changes. On the contrary, the unaffected base metal or simply known as the parent metal is the region that has not experienced microstructural changes [11].

The effects of microstructure towards weld corrosion have been published in many researches. A study by Lee, Bond and Woollin [3], has concluded that increasing

hardness, grain size, level of aligned second phase and decreasing level of microstructure refinement may increase preferential weld corrosion. Preferential weld corrosion is often associated with HAZ region due to the hard structures of bainite and martensite formation [2].

A study by Avendano-Castro et.al [12], localized weld corrosion will be a huge threat when the small area of weld metal and HAZ become anodic to the parent metal. This is known as the galvanic effects which normally occur due to the difference in microstructures and compositions of the weldment regions resulting from the cooling and heating of metals during welding process [1]. According to Turgoose, Palmer and Dicken [2], Manual Metal Arc (MMA) welding will cause weld metal to heavily deoxidized through the coating, thus resulting in a fine dispersion of small oxides in the molten metal. The small oxides act as nucleation sites for acicular, long and narrow ferrite, producing a tough weldment. However, they stated that the inclusions and the increase in manganese and silicon contents can lead to rapid weld metal corrosion. Similarly, Tungsten Inert Gas (TIG) welding will cause an increase of silicon to the wire to ensure weld metal fluidity. The silicon forms silicon oxide inclusions which act as corrosion initiation sites.

2.3 Carbon Dioxide (CO₂) Corrosion

Carbon dioxide corrosion is the most predominant form of corrosion faced in oil and gas industry. Dissolved carbon dioxide is very corrosive to carbon steel and low alloy steels pipes as well as the process equipment in the industry. Due to this fact, corrosion prevention and control costs are very high, which mainly related to material replacement and corrosion control programs. A study by Lopez et al. [13] emphasized that carbon dioxide corrosion not only produce general uniform corrosion, but also localized corrosion which is a very serious problem.

The effects of PWC in CO₂ corrosion have been studied widely by Waard and Milliams [14]. In the presence of water, carbon dioxide gas will dissolves to form aqueous carbonic acid which can further dissociates and become corrosive to the steel [13] [14].

Carbon dioxide dissolves in water to form carbonic acid as shown in Equation 1:



Carbonic acid ionizes to form hydrogen ion and bicarbonate ion as shown in Equation 2:



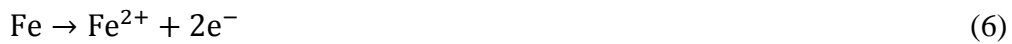
The bicarbonate ion further ionizes to form hydrogen ion and carbonate ion as shown in Equation 3:



In CO₂ corrosion, the possible cathodic reactions are determined by the amount of CO₂ gas in the system as shown in Equation 4 and the pH level of the system as shown in Equation 5:



The anodic reaction for metal degradation in CO₂ corrosion is shown in Equation 6:



The overall equation is shown in Equation 7:



According to Nesic et.al [15], the formation of iron carbonate precipitate, FeCO₃ can occur when the concentrations of Fe²⁺ and CO₃²⁻ ions have exceeded their solubility limit. FeCO₃ precipitates that forms on the pipe wall surface helps to reduce the corrosion process by blocking the underlying steel portion from further dissolution. In addition, the formation of this protective layer is usually favorable at elevated temperature as mentioned by Popoola et.al [6]. Surprisingly, researches [6] [15] claimed that the metal can also starts to corrode under the protective layer. Thus, there are many different parameters that should be taken into account when studying CO₂ corrosion, as explained below.

2.3.1 The Effect of pH on CO₂ Corrosion

In CO₂ corrosion, as the pH level increases, the uniform corrosion rate decreases [13] due to the formation of bicarbonate and carbonate salts as shown in Equation 2 and Equation 3. Netic's publication [15] concluded that high pH level results in a decreased solubility of iron carbonate, increased super saturation, and consequently results in higher precipitation rate and surface scaling.

2.3.2 The Effect of Temperature on CO₂ Corrosion

Temperature plays significant role in the formation of FeCO₃ precipitate. According to Nazari et.al [16], the formation of iron carbonate layer depends on two simultaneous phenomena which are; the corrosion of steel and the precipitation of iron carbonate. Increasing the temperature will increase the corrosion rate because high temperature accelerates the diffusion of species during electrochemical reactions. However, the iron carbonate solubility limit decreases with increasing temperature. His experiment showed that the iron carbonate film was not formed at 55°C because of higher corrosion rate compared to precipitation rate, but the iron carbonate layer formed at 65°C. He concluded that the optimum temperature for the solubility to decrease sufficiently to cause precipitation of iron carbonate film is at temperature 65°C.

2.3.3 The Effect of Acetic Acid (HAc) on CO₂ Corrosion

The effect of acetic acid on CO₂ corrosion has been studied extensively by many authors [5] [7] [8] [9]. Acetic acid is a weak acid since it dissociates partially in water. A study by Gunaltun et.al [9] discussed about the presence of acetic acid, HAc in CO₂ corrosion especially at top line transportation where wet gas experience significant heat exchange causing water vapor carried by the wet gas to condense on the pipe wall. HAc dissociates into hydrogen and acetate ions [17] as shown in Equation 8:



The same study [9] also reveals that the HAc dissociation can occur rapidly. The increase in free hydrogen ions formed from the dissociation will further decrease the pH and solubilizing ferrous ions. Thus, reduction of iron carbonate films thickness will occur, in addition of increasing rate of cathodic reaction [5] [9].

George [8] explained that HAc may be the main source of hydrogen ions since it is a stronger acid compared to carbonic acid. The acetate ions from the reaction in Equation 8 will form causing in the formation of iron acetate as shown in Equation 9.



In contrast with the solubility of iron carbonate precipitate, iron acetate's solubility is much higher. Thus, the formation of protective film by iron acetate does not occur readily, which results in the increase of corrosion rate of steel [9].

CHAPTER 3: METHODOLOGY

3.1 Research Methodology

The execution of this project is according to the following research methodology:

3.1.1 Sample Preparation

A weldment specimen is taken from API 5L X52 carbon steel which had been welded with single-v butt weld. The weldment sample is cut into three regions comprising of parent metal region, HAZ region and weld metal regions. All the sectioned samples are grinded and polished with 180 grit, 320 grit, 400 grit, 600 grit sandpapers and polished with diamond suspension. The set of samples is dedicated for electrochemical test using glass cell setup.

3.1.2 Microstructure Analysis

Weldment segment is cut from the pipeline regions, polished and etched with Nital in order to expose the three weld regions microstructures. Then, they are polished with diamond suspension to produce a mirror-like surface finish. The microstructures of these regions will be investigated under Optical Microscope (OM).

3.1.3 Corrosion Test and Corrosion Monitoring Analysis

A glass cell is set up to perform Linear Polarization Resistance monitoring. LPR is used to calculate corrosion rate by applying over potential to the equilibrium electrode potential. The glass cell setup is placed on a hot plate as a source of heat to increase the temperature up to 60°. Then, the solution is purged with carbon dioxide gas throughout the whole experiment period. An auxiliary electrode and a reference electrode are used with the three metal samples mounted together as working electrode. Zero Resistance Ammeter (ZRA) is used to analyze the corrosion current behavior of each metal.

3.2 Project Workflow

Project workflow for FYP I and FYP II are as illustrated in Figure 3.1.

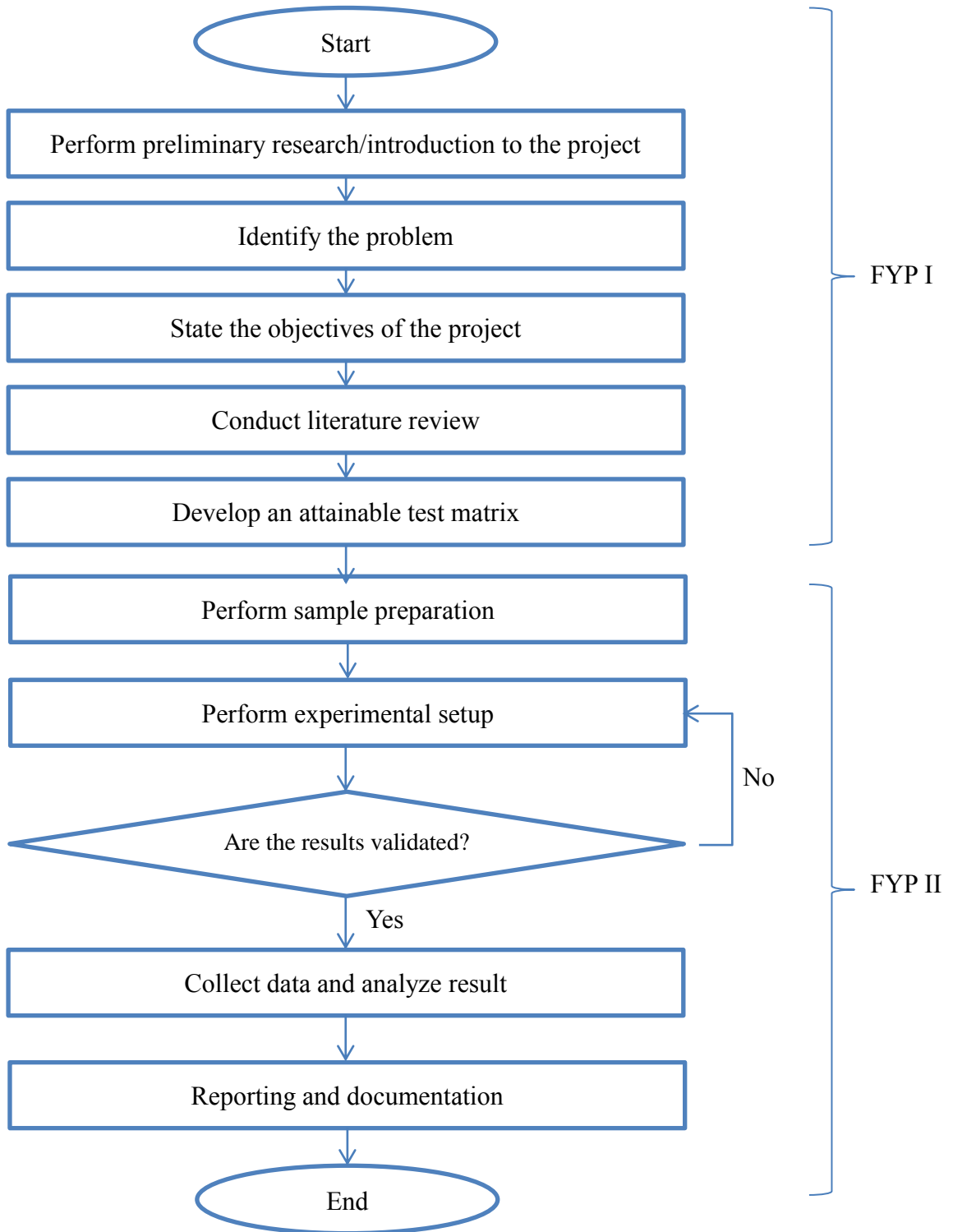


FIGURE 3.1. Project flow chart.

3.3 Gantt Charts and Key Milestones

The timeline for this project is divided into FYP I and FYP II. Table 3.1 shows the Gantt chart for FYP I and Table 3.2 shows the Gantt chart for FYP II.

TABLE 3.1. FYP I Gantt chart.

Agenda / Week	FYP I						
	1-2	3-4	5-6	7-8	9-10	11-12	13-14
Topic selection							
Literature review <ul style="list-style-type: none"> • Understanding material & weldment structure • Understanding CO₂ corrosion and HAc corrosion 							
Develop Test matrix <ul style="list-style-type: none"> • Understanding LPR and WL techniques 							
Submission of extended proposal			•				
Proposal defense presentation				•			
Project work continues <ul style="list-style-type: none"> • Familiarizing with process of sample preparation • Understanding experimental setup • Gathering pipe material 							
Submission of interim draft report						•	
Submission of interim report							•

• Key milestones

TABLE 3.2. FYP II Gantt chart.

Agenda / Week	FYP II						
	1-2	3-4	5-6	7-8	9-10	11-12	13-14
Sample preparation <ul style="list-style-type: none"> • Gathering equipment required • Sectioning and milling process • Grinding, polishing and etching • Conduct microstructural analysis using SEM and OM 							
Experimental setup <ul style="list-style-type: none"> • Conduct Linear Polarization Resistance <ul style="list-style-type: none"> - Solution preparation, electrical setup, open-circuit test, LPR test, cleaning process. 							
Submission of progress report				•			
Collect data and analyze result							
Pre-SEDEX					•		
Submission of draft final report						•	
Submission of dissertation						•	
Submission of technical paper						•	
Viva presentation							•
Submission of project dissertation							•

• Key milestones

3.4 Test Matrix

Table 3.3 shows the general test matrix for glass cell experiments:

TABLE 3.3. Experimental parameters.

Parameters	Value
Temperature	60°C
pH	4 and 6.6
Acetic acid concentration	0 ppm and 1000 ppm
Flow condition	0 rpm
CO ₂ partial pressure	1 bar
NaCl content	3%
Purging gas	CO ₂
Duration	24 hours

The duration of experiment is set for 24 hours for LPR experiment as shown in Table 3.3, as advised in NACE standard. If anticipated corrosion rates are moderate or low which in this case, the expected corrosion rate is more than 2mm/year; the duration of test can be calculated by using Equation 10:

$$\text{Duration of test (h)} = \frac{50}{2 \text{ mm/year}} = 25 \text{ hours} \approx 24 \text{ hours.} \quad (10)$$

All procedures conducted in the experiment must follow the guidelines provided in the following standards:

1. ASTM E3-11 Standard Guide for Preparation of Metallographic Specimens
2. ASTM G5-94 (Reapproved 2004) Standard Reference Test Method for Making Potentiostatic and Potentiodynamic Anodic Polarization Measurements
3. NACE Standard TM0169-2000 Standard Test Method for Laboratory Corrosion Testing of Metals.

3.4.1 Linear Polarization Resistance Experiment

Test matrix 2 : Linear Polarization Resistance Experiment

Objective : To investigate the effects of acetic acid concentration at different temperatures.

Experimental setup : Linear Polarization Resistance

The solution prepared for the experiments were according to the parameters shown in Table 3.4.

TABLE 3.4. Solution parameters.

Run	Temperature (°C)	Acetic acid concentration (ppm)	pH level
1	60	0	4
2	60	1000	4
3	60	0	6.6
4	60	1000	6.6

A set of samples consisting of parent metal (PM), heat-affected zone (HAZ) metal and weld metal (WM) were grinded and polished. Then, the three samples were soldered with three different copper wires. The three samples are placed together in one mould, uncoupled and cold-mounted with epoxy. All sample surfaces were polished again and placed in a solution made according to the parameters shown in Table 3.3 and Table 3.4.

The electrochemical setup was done by preparing the solution according to experiment parameters, then connecting the auxiliary electrode, reference electrode and the mounted samples as the working electrode. The connection was made to the data logging PC. First, the open-circuit potential was recorded during the start of immersion. Then, the Potentiodynamic scan was recorded at a potential sweep rate of $\pm 10\text{mV}$ to record the current continuously. After 24 hours, the data shown in the Sequencer software were recorded. All electrical and gas connections were disconnected properly before the test apparatus were cleaned. The same procedures were repeated according to the parameters of Run 2, Run 3 and Run 4 shown in Table 3.4.

3.5 Sample Preparation

The initial sample was obtained from an old X52 pipeline that had been exposed to CO₂ corrosion. A weldment part of the pipeline is shown in Figure 3.2.



FIGURE 3.2. Original sample of X52 weldment.

The weldment was milled using vertical turret milling machine to produce flat surface. Then, it was grinded up to 600 grit and polished with diamond suspension particle. The sample was then etched with Nital revealing discrete color gradient indicating different regions of parent metal, HAZ metal and weld metal as shown in Figure 3.3.

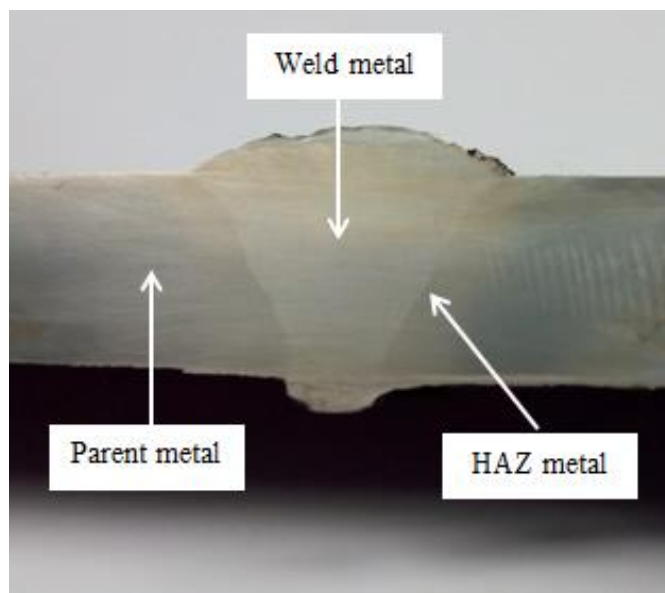


FIGURE 3.3. Parent metal, HAZ metal and weld metal regions of a weldment.

Next, the regions are marked and sectioning was done to separate the regions as shown in Figure 3.4.



FIGURE 3.4. Parent metal, HAZ metal and weld metal after sectioning process.

In order to perform electrochemical test, the samples need to be cold mounted. The area of metals is shown in Table 3.5.

TABLE 0.5. Area of parent metal, heat affected zone metal and weld metal.

Metals	Area (cm ²)
Parent metal (PM)	0.8 cm ²
Heat affected zone metal (HAZ)	0.38 cm ²
Weld metal (WM)	0.51 cm ²

Figure 3.5 shows the mounted samples of the three metals to be used as working electrodes in the electrochemical test. The three metals are mounted separately in epoxy mixture and left overnight to harden.

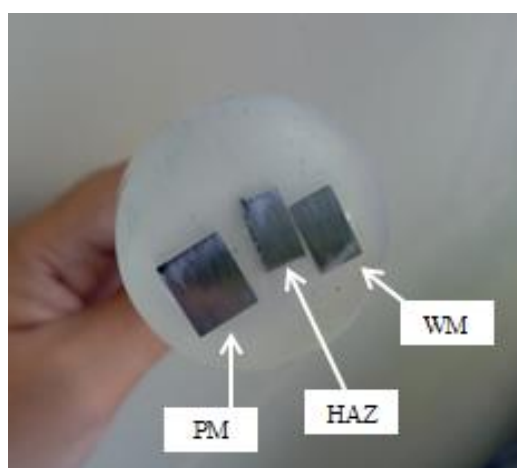


FIGURE 3.5. Mounted samples of the working electrodes.

The electrochemical setup was done as shown in Figure 3.6. Once the solution was prepared, it was purged with carbon dioxide gas for about 40 minutes and placed on a hot plate. A thermometer was placed to ensure that the temperature was kept constant at 60°C. Then, the auxiliary electrode, reference electrode and the working electrode which contained the three metals mounted together were carefully placed into the solution and sealed properly. The connections of auxiliary electrode and reference electrode were clipped accordingly. The copper wire connected to the parent metal was clipped to the connection labeled WE1 (which stands for working electrode 1). The HAZ metal and weld metal were connected to the wire labeled Z2 and Z3 respectively. Finally, the connections were connected to the ACM Gill AC equipment to be recorded in a data logging computer.

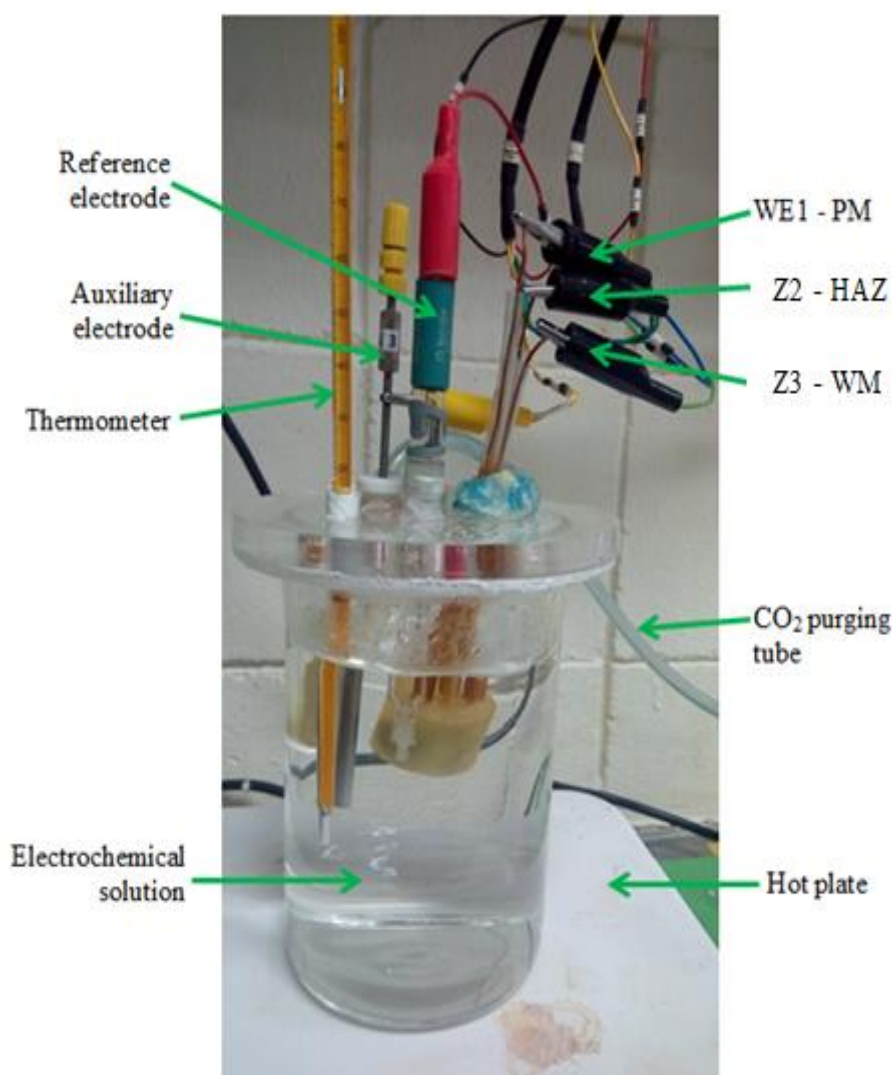


FIGURE 3.6. The electrochemical setup.

3.6 Solution Preparation

The solution made for electrochemical test is according to the test parameters as shown in Table 3.3 and Table 3.4. The following equations were used to calculate the amount of sodium chloride and acetic acid required.

3.6.1 Calculation for 3 wt% NaCl Required

1 ppm stands for one part per million.

$$1 \text{ ppm} = 1 \text{ mg/l}$$

$$1 \% \text{ from } 1\,000\,000 \text{ parts: } \frac{1}{100} \times 1\,000\,000 = 10\,000 \text{ ppm}$$

$$\text{Thus, } 3 \text{ wt \% equals to } = \frac{3}{100} \times 1\,000\,000 = 30\,000 \text{ ppm}$$

As mentioned earlier, 1 ppm equals to 1 milligram per litre, thus:

$$3\% \text{ NaCl} = 30\,000 \text{ ppm} \times 10^{-3} = 30 \text{ g/l}$$

3.6.2 Calculation for 1000 ppm Acetic Acid Required

$$1 \text{ ppm} = \frac{1 \text{ l}}{1\,000\,000} = \frac{1\,000 \text{ ml}}{1\,000\,000} = 1 \times 10^{-3} \text{ ml}$$

$$1000 \text{ ppm} = 1\,000 \times (1 \times 10^{-3} \text{ ml}) = 1 \text{ ml}$$

CHAPTER 4: RESULT AND DISCUSSION

4.1 Microscopy Analysis

Figure 4.1, Figure 4.2 and Figure 4.3 show the microstructure of parent metal, heat affected zone metal and weld metal respectively. These figures are taken at 20 times magnification using optical microscope. From the parent metal microstructure shown in Figure 4.1, the large grain boundaries can be clearly seen. This is different compared to weld metal and heat affected zone metal which has very fine and small grain boundaries. The reason is due to the fact that heat affected zone metal and weld metal have both experienced heating during welding which causes strain hardening. The heating in heat affected zone causes the formation of bainite or martensite from original ferrite microstructure. Thus the grain boundaries become smaller and the heat affected zone metal and weld metal can be clearly differentiated from parent metal.

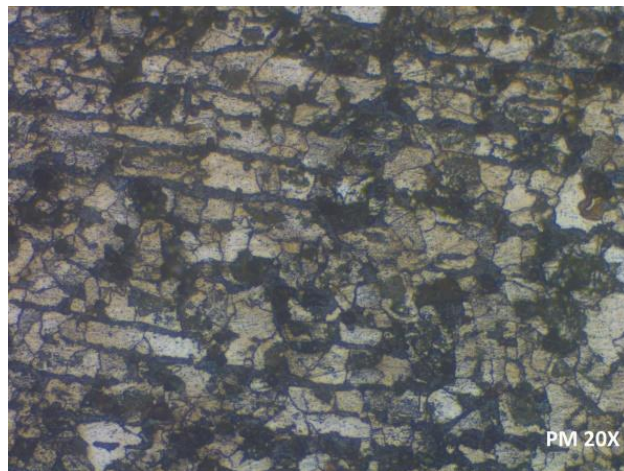


FIGURE 4.1. Microstructure of parent metal at 20X magnification.

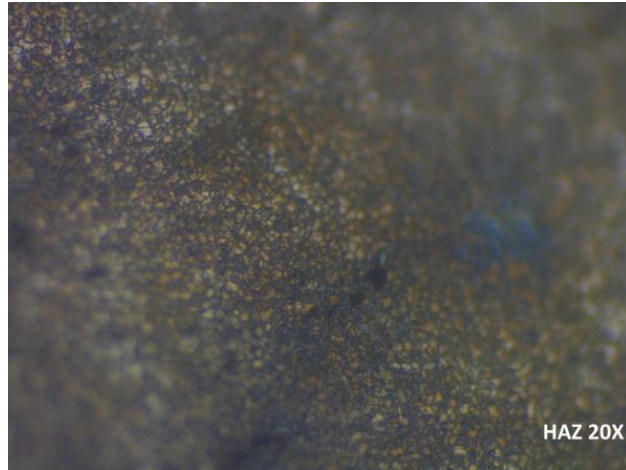


FIGURE 4.2. Microstructure of HAZ metal at 20X magnification.

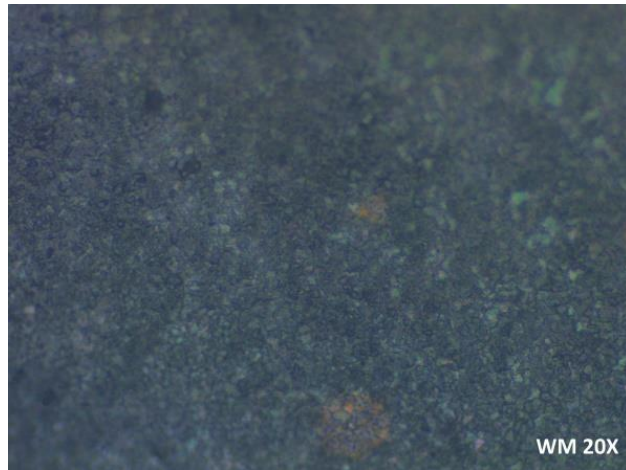


FIGURE 4.3. Microstructure of weld metal at 20X magnification.

4.2 Corrosion Currents of Parent Metal, HAZ Metal and Weld Metal

The corrosion current (I_{corr}) are recorded throughout the 24 hour period and used to calculate the corrosion rate.

Figure 4.4 shows two graphs plotting the corrosion current (I_{corr}) versus time in 0 ppm and 1000 ppm acid at pH 4.

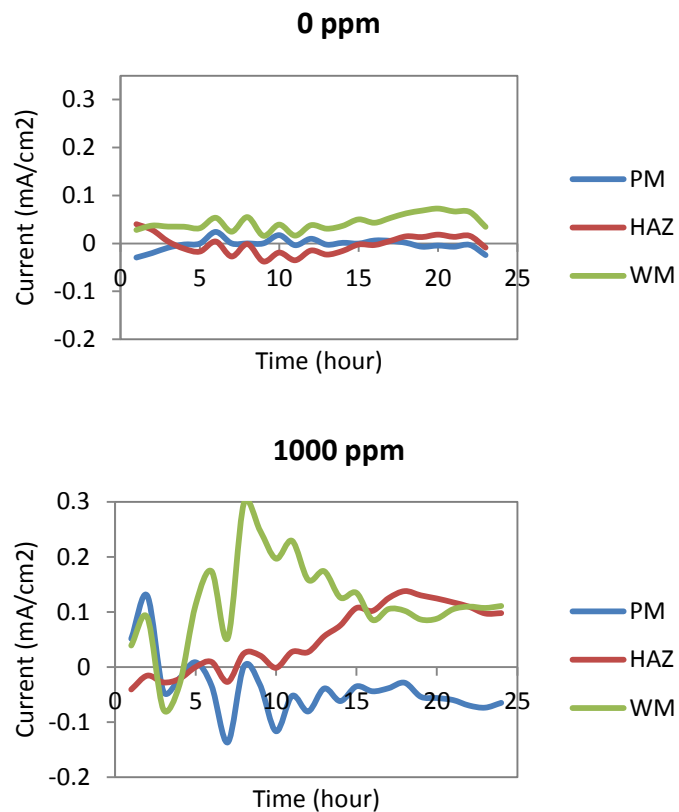


FIGURE 4.4. I_{corr} versus time in 0 ppm and 1000 ppm acid at pH 4.

The positive values of I_{corr} indicate anodic behavior while negative values indicate cathodic behavior. Figure 4.4 shows that weld metal has highest anodic currents with and without the present of acetic acid at low pH (pH 4). This means that weld metal experienced more metal lost compared to heat affected zone metal and parent metal.

Figure 4.5 shows two graphs plotting the corrosion current (I_{corr}) versus time in 0 ppm and 1000 ppm acid at pH 6.6.

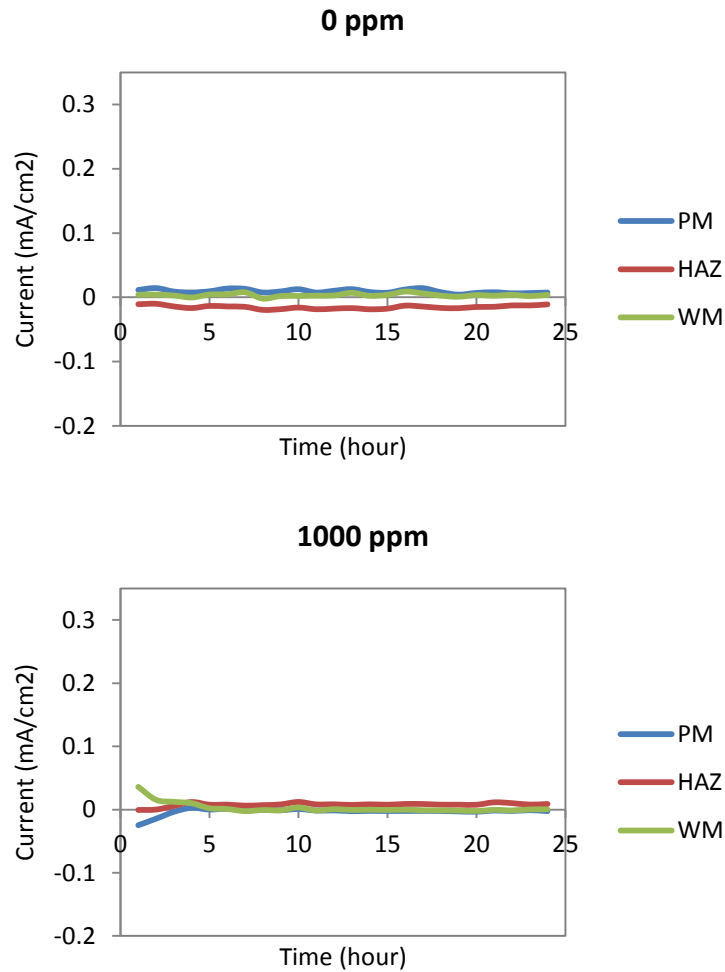


FIGURE 4.5. Corrosion current versus time in 0 ppm and 1000 ppm acid at pH 6.6.

Figure 4.5 shows that the corrosion currents for all metals are very low at pH 6.6 in both cases; with and without acetic acid, compared to the corrosion currents recorded at pH 4 as shown in Figure 4.4. However, the corrosion currents of all metals at pH 6.6 are more stabilized and less fluctuated compared to corrosion currents at pH 4. In the absence of acetic acid, the parent metal shows highest anodic behavior followed by weld metal, and the heat affected zone metal behaves cathodically throughout the experiment. In contrast with the currents in the presence of 1000 ppm acetic acid, heat affected zone metal shows highest anodic behavior compared to parent metal and weld metal. Both parent metal and weld metal have almost similar corrosion currents throughout the experiment.

4.3 Corrosion Rates of Parent Metal, HAZ Metal and Weld Metal

The following section will discuss about the trend of corrosion rates for the three weldment regions namely parent metal, HAZ metal and weld metal.

4.3.1 Corrosion Rates at pH 4 with 0 ppm Acetic Acid

Figure 4.6 shows the corrosion rates of the baseline experiment where no acetic acid was added and the pH was maintained at pH 4.

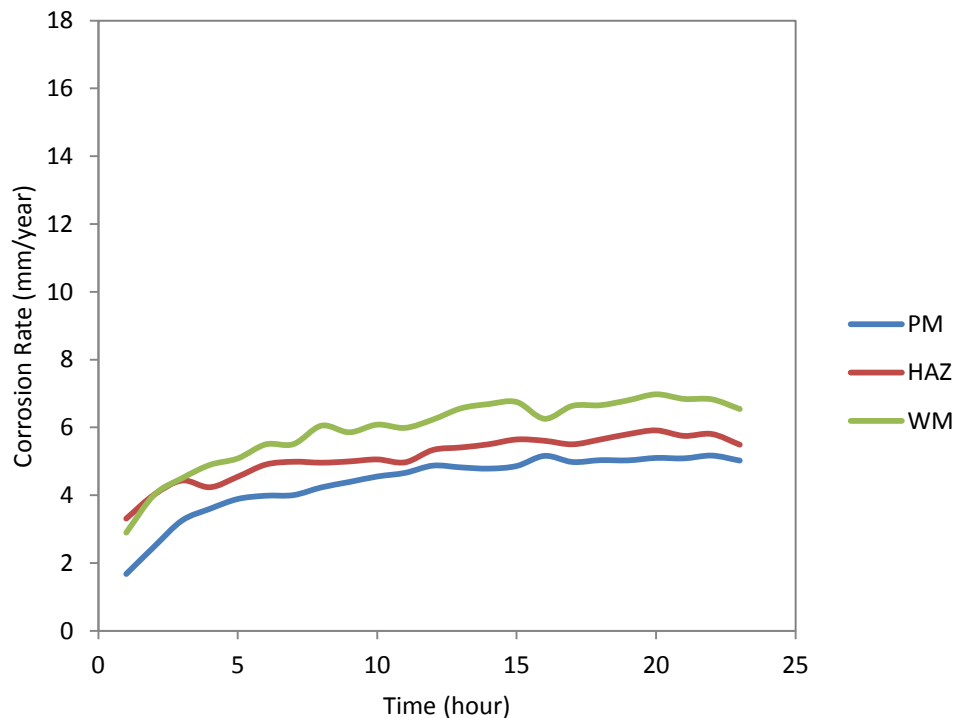


FIGURE 4.6. Corrosion rate versus time at pH 4 with 0 ppm acid.

As the baseline experiment, no acetic acid was added to the solution, thus the concentration of acetic acid in the solution was recorded as 0 ppm. As mentioned in the methodology section, carbon dioxide gas was used to purge the solution in order to prevent contamination of oxygen in the solution. By purging the solution with carbon dioxide gas, the pH was maintained at pH 4 and was monitored throughout the experiment. In case of any increment in pH level, hydrochloric acid was added to the solution to lower the pH level back to pH 4.

Based on Figure 4.6, it shows the corrosion rates for the three metals; parent metal, HAZ metal and weld metal. At the start of the experiment, the corrosion rate for all the three types of metals increased drastically up to the 5th hour and then gradually increased and stabilized towards the end of the experiment. Weld metal showed the highest corrosion rates throughout the hours and reached a maximum of 7.0 mm/year at 20th hour. The second metal that showed highest corrosion rate was the HAZ metal. The maximum corrosion rate achieved by HAZ metal was 5.9 mm/year as shown in Figure 4.4. The metal that showed the lowest corrosion rate was the parent metal with maximum corrosion rate of 5.2 mm/year.

The trend of corrosion rates shown in Figure 4.4 was due to the pH level 4. The acidity of the solution inhibits the formation of iron carbonate as a protective film. At low pH level, the solubility rate of iron carbonate is higher than its precipitation rate thus the corrosion rates increased.

4.3.2 Corrosion Rates at pH 4 with 1000 ppm Acetic Acid

Figure 4.7 shows the trend of corrosion rates recorded by parent metal, HAZ metal and weld metal in a solution with 1000 ppm acid at pH 4.

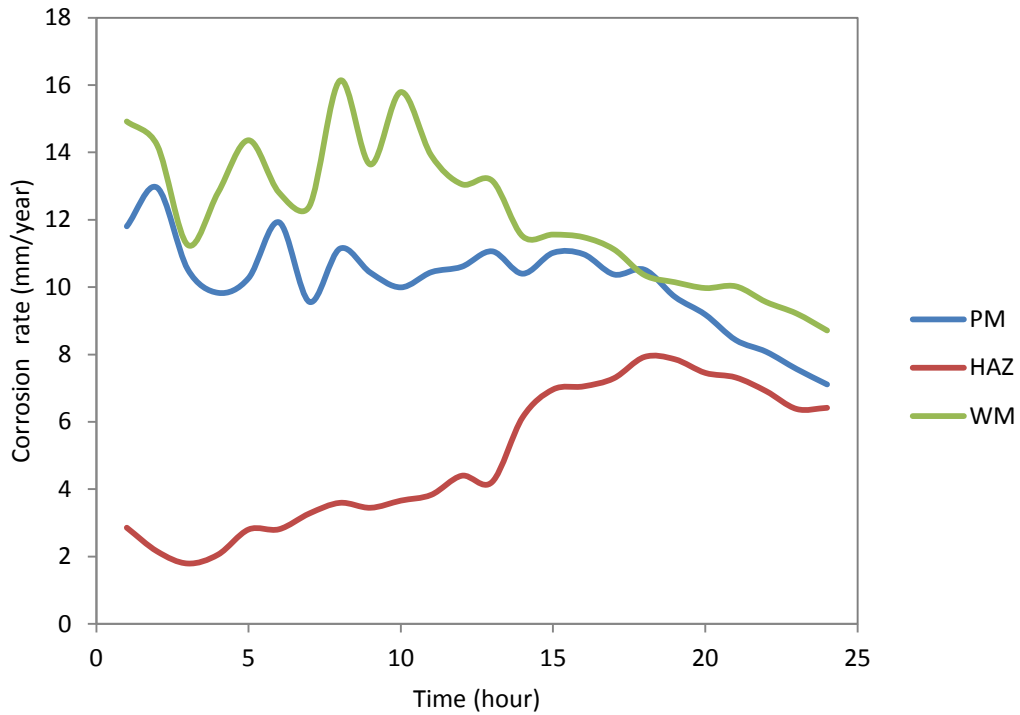


FIGURE 4.7. Corrosion rate versus time at pH 4 with 1000 ppm acid.

In this experiment, the pH level was maintained at pH 4 and 1000 ppm acetic acid was added to the solution. Based on Figure 4.7, at the start of the experiment, the corrosion rate for parent metal and weld metal fluctuated but were stabilized after 15th hour. For the weld metal, the corrosion rate fluctuated between 11 mm/year to 16 mm/year in the first half of the experiment and gradually decreased thereafter up to 9 mm/year.

Similar to the result shown in Figure 4.6, the maximum corrosion rates among the three metals was the weld metal with maximum corrosion rate of 16.1 mm/year. The second highest corrosion rate was recorded by the parent metal which achieved a maximum corrosion rate of 13.0 mm/year. The lowest corrosion rates trend was recorded by the HAZ metal. Unlike the other two metals, corrosion rate for HAZ

metal started at a very low rate, 2.2 mm/year, and then started to increase significantly up to 7.9 mm/year before decreasing slowly to 6.4 mm/year.

In Figure 4.7, the trend of corrosion rates recorded was affected by the pH and acid concentration of the solution. The corrosion rates increased because the low pH inhibits the formation of iron carbonate as the protective film. Moreover, the acidity of the solution was also due to the presence of acetic acid that increased the free hydrogen ions content due to its dissociation.

4.3.3 Corrosion Rates at pH 6.6 with 0 ppm Acetic Acid

Figure 4.8 shows the corrosion rates recorded by the three metals at pH 6.6 in the absence of acetic acid.

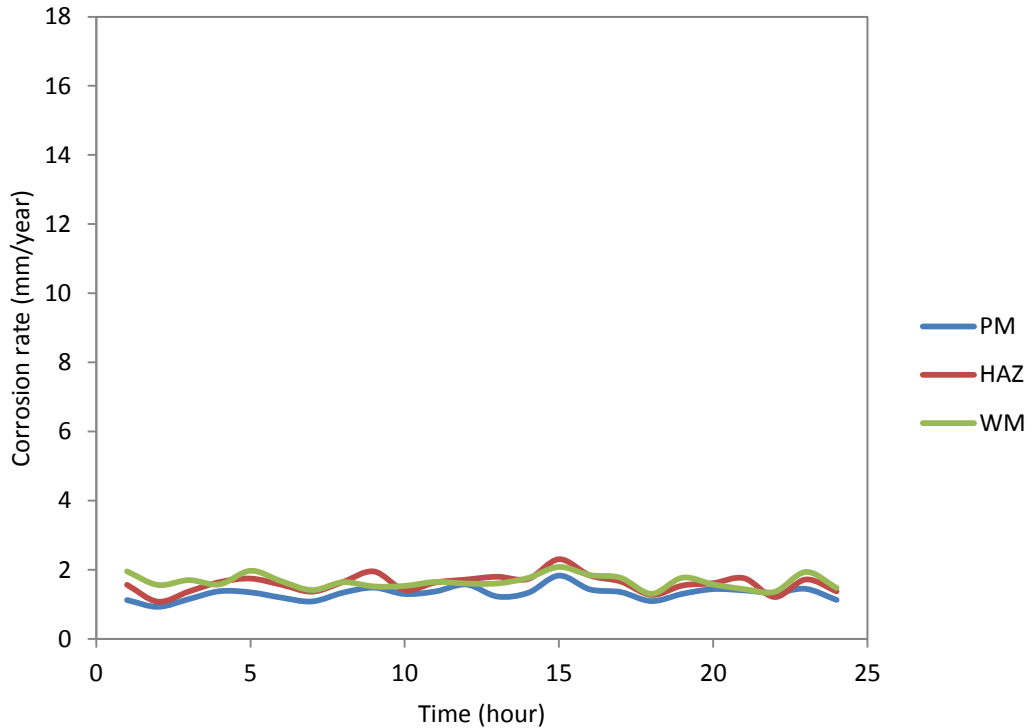


FIGURE 4.8. Corrosion rates versus time at pH 6.6 with 0 ppm acid.

Based on the figure, the corrosion rates of parent metal, heat affected zone metal and weld metal are in the range of 1.0 mm/year to 2.3 mm/year only. All three metals showed quite similar trends of corrosion rates. However, parent metal constantly showed the lowest corrosion rates compared to weld metal and heat affected zone. The fluctuation trends of the corrosion rates for all three metals were uniform throughout the experiment. There was also not much difference of corrosion rates in between the three metals despite the fluctuations. This figure shows that in the absence of acetic acid, the corrosion rates decreased at high pH level. This is due to the fact that there was no acetic acid that contributed to the acidity of the solution. Moreover, the high pH which was closed to neutral made the formation of iron carbonate as a protective layer became favorable. Due to the formation of this protective layer, the corrosion rates were reduced.

4.3.4 Corrosion Rates at pH 6.6 with 1000 ppm Acetic Acid

Figure 4.9 shows the corrosion rates recorded by parent metal, weld metal and heat affected zone metal at pH 6.6 with 1000 ppm acetic acid present in the solution.

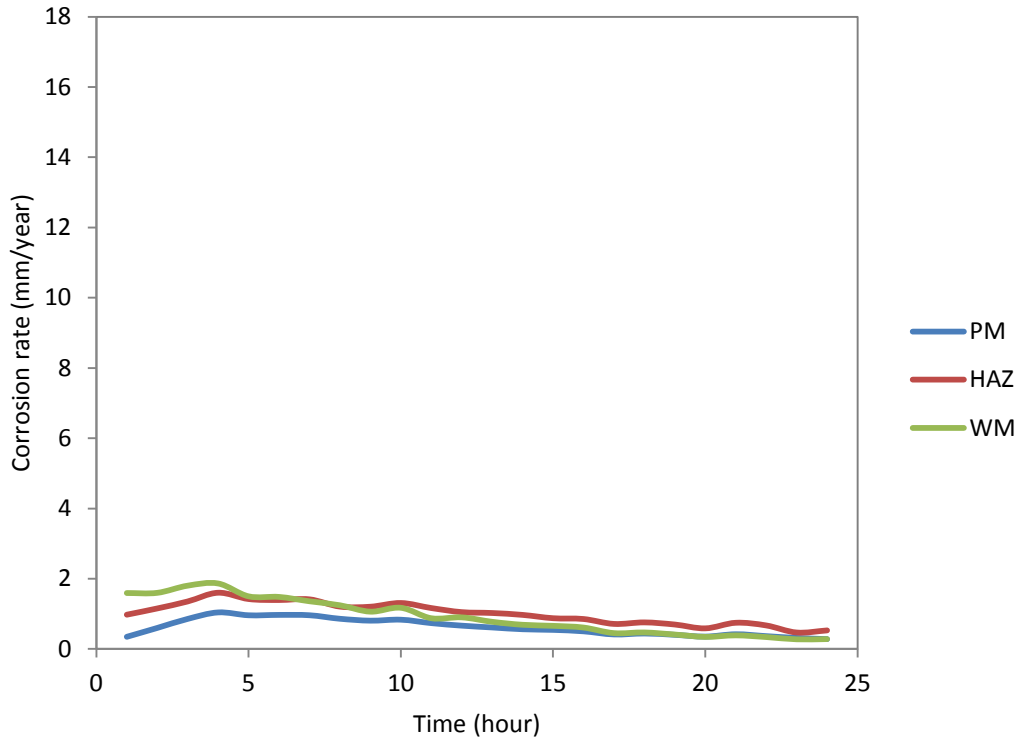


FIGURE 4.9. Corrosion rates versus time at pH 6.6 with 1000 ppm acid.

Based on the figure, all metals showed significant increase in corrosion rates in the first 5th hour of the experiment. Then, the corrosion rates started to decrease towards the end. The range of corrosion rates recorded in Figure 4.9 was from 0.4 mm/year to 1.9 mm/year. This range of corrosion rates was slightly lower, but almost similar to the range showed in Figure 4.8 which was between 1.0 mm/year to 2.3 mm/year. Throughout the experiment, the corrosion rates of all metals did not fluctuated much; however, the trend was uniform for all metals. Heat affected zone showed higher corrosion rates compared to weld metal and parent metal. Towards the end of the experiment, the corrosion rates of all metals reduced to below 0.5 mm/year.

The trend of corrosion rates shown in Figure 4.9 indicates that the corrosion rates decreased at high pH level even in the presence of acetic acid. This conclusion is similar to the trend shown in Figure 4.8 where corrosion rates decreased at high pH level in the absence of acetic acid. The acetic acid present in the solution was neutralized by the sodium hydroxide that was added to the solution to achieve pH 6.6. Thus, the dissociation of acetic acid does not occur and pH was kept constant at pH 6.6. As mentioned earlier, the formation of iron carbonate as the protective film was more favorable in high pH level, thus reducing the corrosion rates.

4.4 The Effect of pH

As mentioned in the methodology section, the effect of pH is studied by varying the pH level at pH 4 and pH 6.6. The following section will discuss about the corrosion rates trend at pH 4 and pH 6.6 with and without the present of acetic acid.

4.4.1 The Effect of varying pH at 0 ppm Acetic Acid

Figure 4.10 shows the comparison of corrosion rates of the metals at pH 4 and pH 6.6 in the absence of acetic acid.

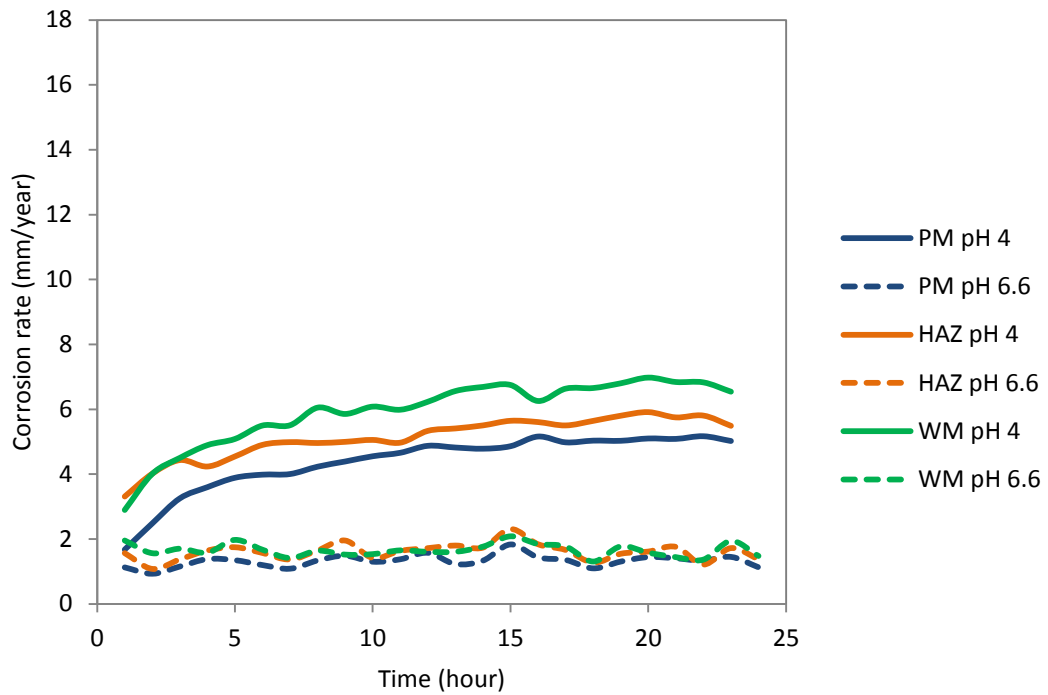


FIGURE 4.10. Corrosion rate versus time for pH 4 and pH 6.6 at 0 ppm acid.

Figure 4.10 shows drastic difference between corrosion rates at pH 4 and pH 6.6. At pH 6.6, the corrosion rates of all metals were extremely low compared to the corrosion rates at pH 4. This trend was constant for all types of metals which proved that the pH affects all the three types of metals, increasing the corrosion rate when pH was low.

The high corrosion rate at low pH means that the corrosion rate was high in acidic medium even though there was no acetic acid present in the solution. The acidity of the solution was solely caused by purging carbon dioxide gas. The carbon dioxide dissolved in water to release hydrogen (H^+) ions. At low pH, the concentration of H^+ ions was high and causes high corrosion rate. High acidity level also inhibits the formation of protective films which consequently cause high corrosion rates.

In order to achieve pH 6.6, sodium hydroxide was added to the solution. At high pH (pH 6.6), the corrosion rates for all metals fluctuated between 1.0 mm/year to 2.0 mm/year only. In fact, Nestic's publication on 2003 [15] concluded that high pH level results in a decreased solubility of iron carbonate, increased super saturation, and consequently results in higher precipitation rate and surface scaling. Thus, the reason of low corrosion rate at high pH level was due to the increase in formation of protective film layer that was able to reduce the corrosion rate. Since the temperature of the experiment was elevated up to 60°C, the formation of protective layer becomes more favorable.

4.4.2 The Effect of varying pH at 1000 ppm Acetic Acid

Figure 4.11 shows the comparison of corrosion rates of the metals at pH 4 and pH 6.6 in the presence of 1000 ppm acetic acid.

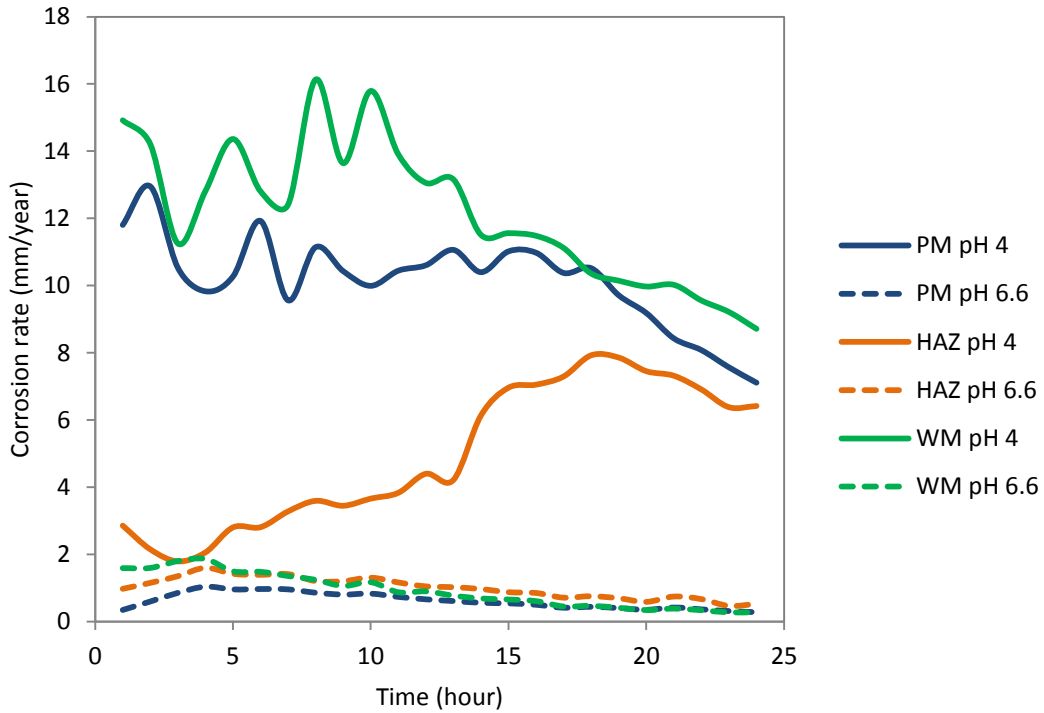


FIGURE 4.11. Corrosion rates versus time at pH 4 and pH 6.6 in 1000 ppm acid.

Similar to the effects of varying pH at 0 ppm acid, there was drastic difference between corrosion rate at pH 4 and pH 6.6 as shown in Figure 4.11. Corrosion rates at pH 4 was higher compared to pH 6.6, and the values of corrosion rates at pH 4 were almost doubled in 1000 ppm acid compared to the corrosion rates in 0 ppm acid as shown in Figure 4.10. However, the corrosion rates at pH 6.6 are similar to Figure 4.10 where the values were in the range of 0 to 2 mm/year only. At low pH, the acidity was contributed by the pH level of the solution and the dissociation of acetic acid too, thus the formation of protective film was very unfavorable. Consequently, low acidity causes the increase in corrosion rates. At high pH (pH 6.6), the corrosion rates of all metals were extremely low compared to the corrosion rates at pH 4. High pH indicates low acidity level, providing favorable condition for the formation of protective film. Therefore, the corrosion rates were reduced at pH 6.6.

4.5 The Effect of Acetic Acid Concentration

As mentioned in the literature review section, George [8] explained that HAc may be the main source of hydrogen ions since it is a stronger acid compared to carbonic acid. Acetic acid dissociates to form free H^+ ions. The increase in free hydrogen ions formed from the dissociation will further decrease the pH and solubilizing ferrous ions. Thus, reduction of iron carbonate films thickness will occur, in addition of increasing rate of cathodic reaction [5] [9]. The following figures will discuss more on this matter.

4.5.1 The Effect of varying Acetic Acid Concentration at pH 4

Figure 4.12 shows the comparison of corrosion rates of the metals in solutions containing 0 ppm and 1000 ppm acetic acid at pH 4.

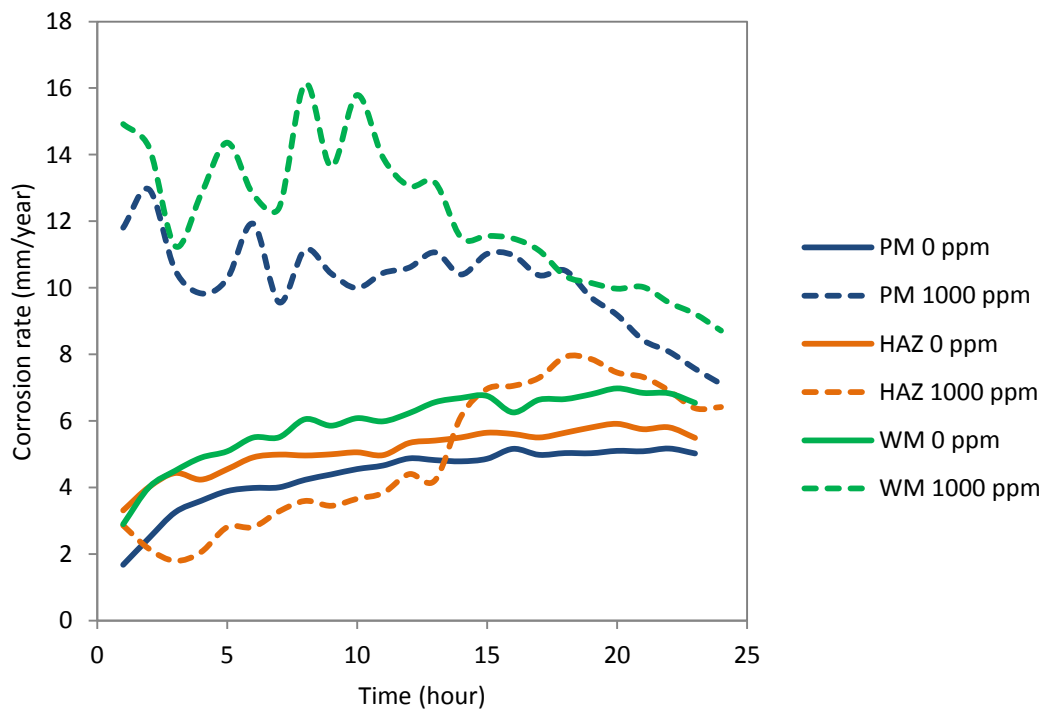


FIGURE 4.12. Corrosion rates versus time with 0 ppm and 1000 ppm acid at pH 4.

Figure 4.12 shows the effect of varying acetic acid at pH 4. Initially there was high difference between corrosion rates for both experiments with and without acetic acid

at pH 4. The corrosion rates at 1000 ppm were between 2 mm/year to 15 mm/year while the corrosion rates at 0 ppm were between 2 mm/year to 3 mm/year. This shows that high corrosion rates were recorded in the presence of acetic acid. However, towards the end of the experiment, the corrosion rates stabilized at almost near to each other.

It can be concluded that the acetic acid increases the corrosion rate of all the three metals at pH 4 due to the fact that without acetic acid the corrosion rate was caused by carbon dioxide only, whereas when acetic acid was added, it increased the corrosion rate due to the acidity caused by dissociation of acetic acid. This fact was supported by previous study done by George [8] which concluded that the acetic acid will act as the main causes of free hydrogen ions, and lowers the precipitation rates of protective films. Consequently, this causes the increase in corrosion rates.

4.5.2 The Effect of varying Acetic Acid Concentration at pH 6.6

Figure 4.13 shows the comparison of corrosion rates of the metals in solutions containing 0 ppm and 1000 ppm acetic acid at pH 6.6.

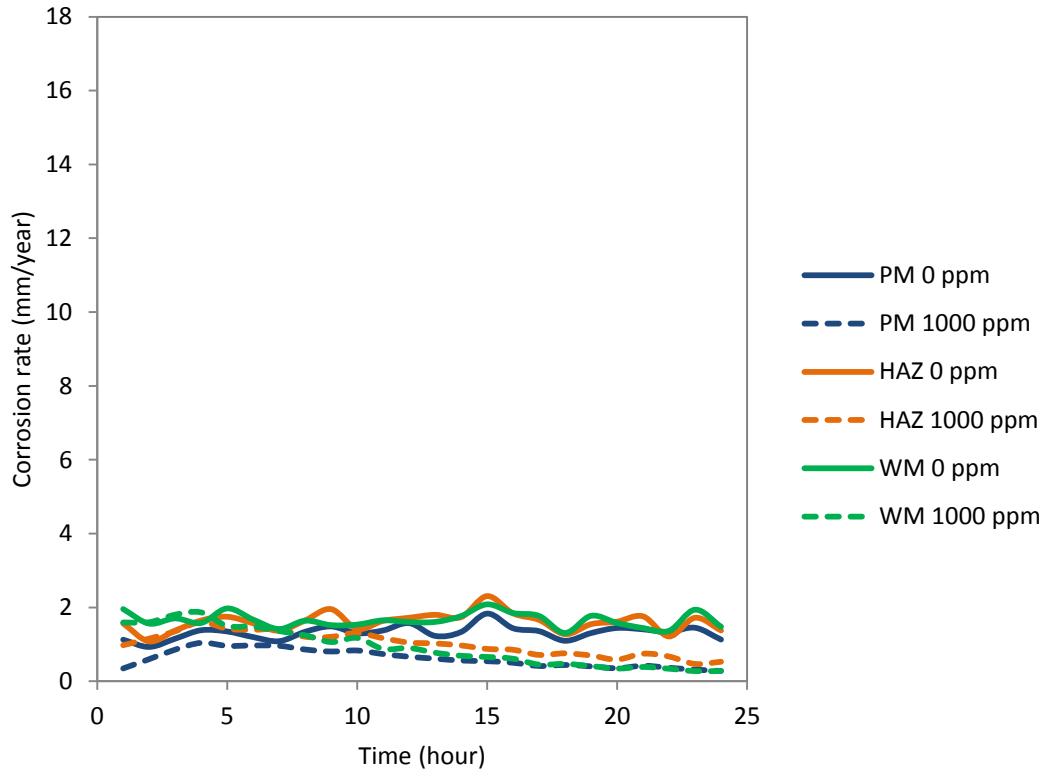


FIGURE 4.13. Corrosion rates versus time in 0 ppm and 1000 ppm acid at pH 6.6.

There was not much difference between corrosion rates at 0 ppm and 1000 ppm acetic acid at pH 6.6 compared to the corrosion rates shown in Figure 4.12. In Figure 4.13, the corrosion rates recorded at pH 6.6 were much lower which was in the range of 0.3 mm/year to 2.0 mm/year only, for both cases with and without acetic acid.

However, Figure 4.13 shows that the corrosion rates are higher in the absence of acetic acid (0 ppm). This means that at high pH (pH 6.6) acetic acid had lower corrosion rates. However, the difference in corrosion rate in with and without acetic acid at pH 6.6 were quite small, about 0.7 mm/year. Even though the acetic acid was present in the solution, it was neutralized by sodium hydroxide solution that was added in the solution to achieve pH 6.6. Therefore, the dissociation of acetic acid did

not occur. Due to the high pH condition, it was more favorable for iron carbonate film to form since its precipitation rate increased at high pH compared to its solubility rate. Therefore the corrosion rates were reduced.

4.6 Summary of Corrosion Rates

In order to clearly see the corrosion rates of parent metal, heat affected zone metal and weld metal in all experiments, Table 4.1 shows the average corrosion rate values and the total average corrosion rates for all metals. Similarly, the data was presented in a bar chart as shown in Figure 4.14.

TABLE 4.1. Summary of corrosion rates.

Experiment	CR PM (mm/yr)	CR HAZ (mm/yr)	CR WM (mm/yr)	Avg CR (mm/yr)
pH 4 0ppm	3.8	5.1	5.9	5.0
pH 4 1000ppm	10.2	4.9	12.2	9.1
pH 6.6 0ppm	1.3	1.6	1.7	1.5
pH 6.6 1000ppm	0.6	1.0	0.9	0.8

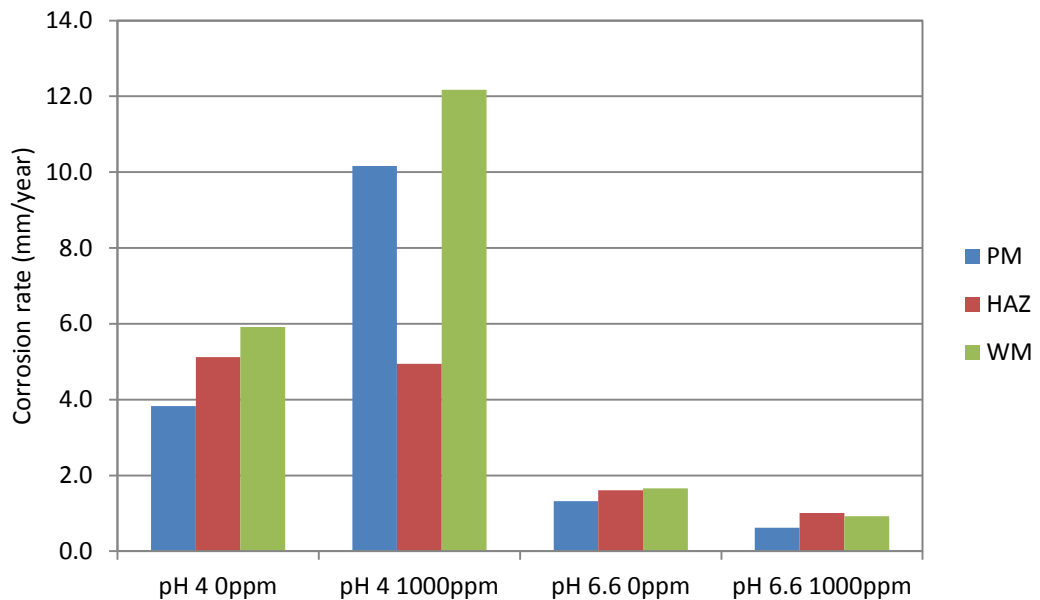


FIGURE 4.14. Summary of average corrosion rates.

Table 4.1 shows the average corrosion rates of all the experiments conducted. Based on Table 4.1, the highest average corrosion rate was recorded from an experiment at pH 4 with 1000 ppm acetic acid present. As discussed earlier, the presence of acid increases the formation of hydrogen ions. Thus, the solution becomes acidic and inhibits the formation of protective layer which causes high corrosion rates.

Figure 4.14 shows the summary of average corrosion rates recorded by the parent metal, heat affected zone metal and weld metal for all the experiments. On average, the highest corrosion rates were recorded by weld metals at almost all conditions, followed by the heat affected zone. The parent metal shows least corrosion rates at almost all conditions. In conjunction with Figure 4.4 and Figure 4.5, the corrosion currents recorded by the Zero Resistance Ammeter showed that the weld metal and heat affected zone metal always reacted anodically and parent metal reacted cathodically. Therefore, the anodic metals experienced more metal loss and recorded high corrosion rates.

4.7 Error Analysis

All of the experiments were conducted in according to the guidelines stated in the ASTM standards. However, discrepancies in the data might occur due to some possible errors in the study. The data required from the glass cell test might be affected by the solution resistance effect caused by the placement of reference electrode and the electrolyte conductivity that can cause the polarization resistance to be overestimated. Moreover, the data recorded by the instrument might be affected by the noise and foreign electronic devices that emit sound wave and electromagnetic waves that could disturb the readings.

CHAPTER 5: CONCLUSION AND RECOMMENDATION

5.1 Conclusion

Based on the experiments conducted, it can be concluded that the weld metal and heat affected zone metal shows high anodic behavior compared to parent metal. Thus the corrosion rates for both metals are higher compared to corrosion rate of parent metal. This fact indicates that the weld metal is very vulnerable to the corrosion of weldment in the presence of carbon dioxide and acetic acid. In oil and gas industry, alloying of weld is one of the solutions implied to shift anodic corrosion of weld metal to the parent metal; however it does not solve the weldment corrosion problem in carbon dioxide and acetic acid corrosion. This is because; the weld metal still behaves anodically in the presence of carbon dioxide and acetic acid corrosion as concluded from this study.

The conclusions derived from this study are:

- At low pH level, the corrosion rates of the weldment metals increased due to the acidity of the solution that inhibits the formation of protective film. Weld metal and heat affected zone metal recorded high corrosion rates compared to parent metal because they behaved anodically.
- At low pH level, the corrosion rates of all metals increased two folds acid due in the presence of acetic acid compared to the corrosion rates recorded in the absence of acetic. The acetic acid dissociates to form more hydrogen ions that further increased the acidity of the solution and caused high corrosion rates.
- At high pH level, the corrosion rates of all metals decreased regardless of the presence of acetic acid. The difference of corrosion rates recorded was in a small range which was between 0 to 2.5 mm/year only. At high pH level, the near-neutral condition was favorable for the formation of protective film. Thus, the corrosion rates were reduced significantly. The presence of acetic acid too brought less effect to the corrosion rates recorded because the acetic

acid was neutralized by sodium hydroxide that was added to the solution in order to achieve pH 6.6.

- At high pH level, the behavior of parent metal, heat affected zone metal and weld metal showed no significant difference. Weld metal behaved anodically whereas the heat affected zone and parent metal interchangeably behaved in anodic and cathodic behaviors.

To conclude, the objectives of this study have been achieved. This study is conducted to understand the behavior of parent metal, heat affected zone metal and weld metal corrosion in the presence of carbon dioxide and acetic acid by understanding the effect of pH level and acetic acid concentration.

5.2 Recommendation

This study was done to investigate the corrosion behavior of weldment regions at varying pH and acetic acid concentrations in carbon dioxide and acetic acid corrosion. The three metals show high corrosion rates in low pH level and in the presence of acetic acid. The extension of this study is recommended to study the effects of pH and acid concentration at much higher acetic acid concentration as the study by Gunaltun and Larrey [9] showed that the concentration of acetic acid in oil and gas pipelines could reach up to 2000 ppm. It is also recommended that the study is conducted for other material types to be able to compare the results as the material used in this study is API 5L X52 carbon steel pipe only.

This study shows that the weld metal and heat affected zone metal recorded high corrosion rates since they behaved anodically in the corrosive system. Therefore, it is recommended to increase the cathodic potential of the weld metal by adding alloying elements in the filler metal during welding process so that the weld metal shall be more cathodic compared to parent metal.

REFERENCES

- [1] B. Richard, X. Hu, and N. Anne, "Assessment of Preferential Weld Corrosion of Carbon Steel Pipework in CO₂-Saturated Flow-Induced Corrosion Environments," in *NACE International Publications Division*, Houston, 2012.
- [2] S. Turgoose, J. W. Palmer, and G. E. Dicken, "Preferential Weld Corrosion of 1% Ni Welds: Effect of Solution Conductivity and Corrosion Inhibitors," in *NACE International Publications Division*, Houston, 2005, p. 2.
- [3] C-M. Lee, S. Bond, and P. Woollin, "Preferential Weld Corrosion: Effects of Weldment Microstructure and Composition," in *NACE International Publications Division*, Houston, 2005, p. 6.
- [4] S. Olsen, B. Sundfaer, and J. Enerhaug, "Weld Corrosion in C-Steel Pipelines in CO₂ Environments-Comparison Between Field and Laboratory Dta," in *NACE International Conferences Division*, Houston, 1997, p. 4.
- [5] P. C. Okafor and S. Nestic, "Effect of Acetic Acid on CO₂ Corrosion of Carbon Steel in Vapor-Water Two-Phase Horizontal Flow," *Chemical Engineering Communications*, vol. 194, no. 2, p. 141, 2007.
- [6] L. T. Popoola, A. S. Grema, G. K. Latinwo, B. Gutti, and A. S. Balogun, "Corrosion Problems During Oil and Gas Production and Its Mitigation," *International Journal of Industrial Chemistry*, vol. 4, no. 35, p. 3, 2013.
- [7] J. L. Crolet, "Role of Free Acetic Acid on the CO₂ Corrosion of Steels," in *NACE International Conferences Division*, Houston, 1999.
- [8] K. S. George, "Electrochemical Investigation of Carbon Dioxide Corrosion of Mild Steel in the Presence of Acetic Acid," Russ College of Engineering and Technology of Ohio University, Ohio, Thesis 2003.
- [9] Y. M. Gunaltun and D. Larrey, "Correlation of Cases of Top of Line Corrosion with Calculated Water Condensation Rates," in *NACE International Conferences Division*, Houston, 2000.
- [10] American Petroleum Institute. (2004, March) Law Resource. Org. [Online]. <https://law.resource.org/pub/us/cfr/ibr/002/api.51.2004.pdf>
- [11] ASM International , "Basic Understanding of Weld Corrosion," in *Corrosion of*

Weldments, Joseph R Davis, Ed. United States of America: ASM International, 2006, ch. 1, pp. 1-10.

- [12] C. Avendano-Castro et al., "Corrosion Kinetics of Pipeline Carbon Steel Weld Immersed in Aqueous Solution Containing H₂S.," *Corrosion Engineering, Science and Technology*, vol. 44, no. 2, pp. 149-156, April 2009.
- [13] D. A. Lopez, T. Perez, and S. N. Simison, "The Influence of Microstructure and Chemical Composition of Carbon and Low Alloy Steels in CO₂ Corrosion. A State-of-the-art Appraisal," *Materials & Design*, no. 24, pp. 561-575, July 2003.
- [14] C. de Waard and U. Lotz, "Prediction of CO₂ Corrosion in Carbon Steel," in *NACE International*, Houston, 1993.
- [15] S. Netic and K. L. J. Lee, "A Mechanistic Model for Carbon Dioxide Corrosion of Mild Steel in the Presence of Protective Iron Carbonate Films - Part 3: Film Growth Model," *Corrosion*, pp. 616-628, July 2003.
- [16] M. H. Nazari, S. R. Allahkaram, and M. B. Kermani, "The Effects of Temperature and pH on the Characteristics of Corrosion Product in CO₂ Corrosion of Grade X70 Steel.," *Materials and Design*, vol. 31, no. 7, pp. 3559–3563, August 2010.
- [17] M. Singer, B. Brown, A. Camacho, and S. Netic, "Combined Effect of CO₂, H₂S and Acetic Acid on Bottom of the Line Corrosion," in *NACE International*, Houston, 2007, pp. 1-25.
- [18] K. Alawadhi and M. J. Robinson, "Preferential Weld Corrosion of X65 Pipeline Steel in Flowing Brines Containing Carbon Dioxide," *Corrosion Engineering, Science and Technology*, vol. 46, no. 4, pp. 318-329, June 2011.